

# Domain Structures in Fourth-Order Phase and Ginzburg-Landau Equations

David Raitt<sup>+</sup>

Hermann Riecke

*Department of Engineering Sciences and Applied Mathematics  
Northwestern University  
Evanston, IL 60208, USA*

In pattern-forming systems, competition between patterns with different wave numbers can lead to domain structures, which consist of regions with differing wave numbers separated by domain walls. For domain structures well above threshold we employ the appropriate phase equation and obtain detailed qualitative agreement with recent experiments. Close to threshold a fourth-order Ginzburg-Landau equation is used which describes a steady bifurcation in systems with two competing critical wave numbers. The existence and stability regime of domain structures is found to be very intricate due to interactions with other modes. In contrast to the phase equation the Ginzburg-Landau equation allows a spatially oscillatory interaction of the domain walls. Thus, close to threshold domain structures need not undergo the coarsening dynamics found in the phase equation far above threshold, and can be stable even without phase conservation. We study their regime of stability as a function of their (quantized) length. Domain structures are related to zig-zags in two-dimensional systems. The latter are therefore expected to be stable only when quenched far enough beyond the zig-zag instability.

October 23, 2018

Running title: Stability of Domain Structures

Submitted to Physica D.

This paper is also available from *patt-sol@xyz.lanl.gov* using *get 9402003* in the subject field.

PACS numbers: 47.20.Ky, 47.20.-k, 05.70.Ln

## I. INTRODUCTION

The formation of steady spatial structures in systems far from equilibrium has been studied in great detail over the past years, the classical examples being Rayleigh-Bénard convection and Taylor vortex flow [1,2]. In quasi-one-dimensional geometries they usually share a common feature: the stable structures that arise after the decay of transients are strictly periodic in space and if they are weakly perturbed they relax *diffusively* back to the periodic state. This relaxation has been investigated experimentally in various systems [3,4,5] and the results agree with theoretical results based on the phase-diffusion equation [6,7,8]. This equation describes the slow dynamics of the local phase, the gradient of which is the local wave number. The structures are generally

stable over a range of wave numbers which is limited (at least) by the Eckhaus instability [9]. The Eckhaus instability is characterized by a vanishing of the phase diffusion coefficient and leads usually to a new stable periodic state with a different wave number. This process involves phase slips, i.e. the destruction (or creation) of one or more roll pairs in convection, say. The Eckhaus instability has been investigated in great detail [10,11,12,13], in particular in Taylor vortex flow [14,15].

Recently, it has been pointed out in theoretical work that a vanishing of the diffusion coefficient does not necessarily invoke a phase slip [16,17,18,19,20]. Instead, under certain conditions, the structure can become inhomogeneous and evolve to a stable domain structure which exhibits different wave numbers in different parts of the system and which does *not* relax to a periodic structure. Such a structure is illustrated in fig.1. The thick line denotes the local wave number and the thin line a typical physical quantity such as the mid-plane temperature in convection.

Experimentally, inhomogeneous structures have been found in a variety of systems. Most of them involve at least one time-dependent structure, e.g. counterpropagating traveling waves (or spirals) [21,22], (turbulent) twist vortices amidst regular Taylor vortices [23], localized traveling-wave pulses in binary-mixture convection [24] and steady Turing patterns amidst chemical traveling waves [25]. Recently, however, domain structures involving only steady convection rolls of two different sizes have been observed in Rayleigh-Bénard convection in a very narrow channel [26]. It has been suggested that these structures may be related to the phase-diffusion mechanism discussed above [16].

Similar phenomena are relevant in two-dimensional systems. There, roll (or stripe) patterns usually undergo an instability at small wave numbers in which the phase-diffusion coefficient for perturbations *along* the rolls goes through zero. This leads to an undulatory deformation of the rolls which can grow into a zig-zag pattern. Such patterns are related to domain structures with the ‘zigs’ corresponding to domains of one wave number and the ‘zags’ corresponding to domains of a different wave number.

Here we investigate steady domain structures from two points of view. For structures well above threshold a description of domain structures is obtained using the

appropriate 4th-order phase equation introduced earlier [16,17]. In sec.II we perform a detailed study of this equation. We emphasize the bifurcation that leads to the domain structure and its connection to the Eckhaus instability. These results are compared with recent experiments [26].

Domain structures can also form close to threshold if the basic state becomes unstable to two periodic patterns with different wave numbers. If these two patterns arise at similar values of the control parameter, the resulting competition can be described by a Ginzburg-Landau equation. In sec.III we introduce and investigate the appropriate equation. We present a detailed analysis of the stability regime of domain structures for periodic boundary conditions. In part of the parameter regime they can again be described by the above phase equation. Surprisingly, we find no trace of the breakdown of the phase equation in the stability behavior of the domains. In fact, the domains can be stable even if the local wave number is well below the neutral curve, where the phase equation clearly does not apply.

Within the phase equation, domain structures are only stable if the total phase, i.e. the total number of cells, is conserved. In sec.IV we therefore study the Ginzburg-Landau equation with a spatially ramped control parameter which allows the total phase to change. We find stable domain structures even in this general case and explore their regime of existence. In sec.V we briefly address the relevance of our results to two-dimensional patterns and discuss the zig-zag instability and the stability of the resulting zig-zag patterns in isotropic systems, e.g. Rayleigh-Bénard convection and Turing structures [28], and in anisotropic systems like electroconvection in nematic liquid crystals [29].

## II. DOMAIN STRUCTURES WITHIN THE PHASE EQUATION

In this section we consider steady one-dimensional periodic structures away from threshold. The slow dynamics of long-wavelength perturbations of such structures can be described by an equation for the local phase of the structure. To derive the phase equation one assumes the structure to be close to periodic and expands the relevant fields, e.g. the fluid velocity, according to

$$v(x, t) = v_0(\epsilon^{-1}\varphi(X, T)) + \epsilon v_1(\epsilon^{-1}\varphi(X, T)) + h.o.t., \quad (1)$$

where the slow variables  $X = \epsilon x$  and  $T = \epsilon^2 t$ ,  $\epsilon \ll 1$  have been introduced [1]. Inserting this expansion into the basic equations, e.g. the Navier-Stokes equation, yields at  $O(\epsilon)$  the solvability condition

$$\partial_T \varphi = \mathcal{D}(q, R) \partial_X^2 \varphi. \quad (2)$$

Note that the phase equation (2) is nonlinear through the dependence of the diffusion coefficient on the local

wave number  $q = \partial_X \varphi$ . In addition, we have indicated the dependence of  $\mathcal{D}$  on a control parameter, such as the Rayleigh number  $R$  in convection. As long as the diffusion coefficient  $\mathcal{D}(q, R)$  is positive, perturbations decay diffusively and the structure is stable with regard to long-wavelength perturbations.

If  $\mathcal{D}(q, R)$  becomes negative the structure loses stability and perturbations in the local wave number grow. Usually this leads to a phase slip and eventually to a periodic state with a different wave number. If, however,  $\mathcal{D}(q, R)$  becomes negative in the center of the band of stable wave numbers, the perturbations can saturate and a domain structure arises. This is quite naturally the case when the neutral curve has two minima (see secs.III,IV below) [17,27]. It can, however, even occur if the neutral curve has a single minimum [17,18].

To ensure well-posedness of the phase equation for  $\mathcal{D}(q, R) < 0$  it is necessary to retain higher order derivatives. Introducing an additional slow time  $\tau = \epsilon^4 t$  and expanding the phase around a spatially periodic structure with wave number  $q_0$ ,  $\varphi(X, \tau) = q_0 X + \epsilon \phi(X, \tau)$ , one obtains

$$\partial_\tau \phi = (D + E \partial_X \phi + F (\partial_X \phi)^2) \partial_X^2 \phi - G \partial_X^4 \phi, \quad (3)$$

where

$$\begin{aligned} \epsilon^2 D &= \mathcal{D}(q_0, R), & \epsilon E &= \partial_q \mathcal{D}(q_0, R), \\ F &= \partial_q^2 \mathcal{D}(q_0, R), & G &> 0. \end{aligned} \quad (4)$$

In anticipation of the situation relevant to this paper, we assume  $D$ ,  $E$ , and  $F$  to be  $\mathcal{O}(1)$ . These coefficients can also be determined in a linear stability analysis of the periodic state from the behavior of the growth rate at small values of the Floquet parameter (cf. (20) below). The wave number  $Q = \partial_X \phi \equiv (q - q_0)/\epsilon$  satisfies

$$\partial_T Q = \partial_X^2 (DQ + \frac{E}{2} Q^2 + \frac{F}{3} Q^3 - G \partial_X^2 Q). \quad (5)$$

This equation is the Ginzburg-Landau equation for a conserved order parameter  $Q$  [31]. The static solutions to (5) are most easily understood by rewriting the right-hand side as the equation for a particle in a potential,

$$\begin{aligned} \partial_X^2 Q &= -\partial_Q U(Q), \\ U(Q) &= -\frac{D}{2G} Q^2 - \frac{E}{6G} Q^3 - \frac{F}{12G} Q^4 + CQ \end{aligned} \quad (6)$$

with the integration constant  $C$ . Usually  $\mathcal{D}(q)$  is concave downward implying  $F < 0$ . This yields a potential as sketched in fig.2a, which allows two kinds of solutions. The three extrema correspond to spatially periodic structures, of which only the maximum yields a stable solution within the full equation (3). In addition, there exists a family of unstable, oscillating (in  $X$ ) solutions, which correspond to structures with spatially modulated wave numbers. It contains, as a limiting case, a homoclinic orbit which describes a system with a localized ‘dip’ (or

‘hump’) in the wave number and an associated amplitude depression [10]. By contrast, if  $F > 0$  (fig.2b) two maxima are possible allowing also a heteroclinic orbit connecting two *stable* periodic structures. In this paper we concentrate on such solutions.

The connection between the different solutions is revealed by a bifurcation analysis close to the onset of the instability of the periodic structure. Since (6) can be solved exactly in terms of elliptic integrals it is possible to perform the expansion in the exact solution. This approach emphasizes the importance of phase conservation and is demonstrated in [32].

It is easier, however, to expand the phase in (3)

$$\phi = \eta A_1 e^{iPX} + \eta^2 (A_2 e^{iPX} + B_2 e^{2iPX}) + h.o.t. + c.c. \quad (7)$$

and derive an evolution equation for  $A_1$ . Here  $P = \frac{2\pi}{L} \cdot n$ ,  $n$  integer, and the amplitudes depend on the slow time  $\hat{T} = \eta^4 t$ ,  $\eta \ll 1$ . No term independent of  $X$  arises in (7) because (3) is invariant under  $\phi \rightarrow \phi + const$ . At fifth order one obtains

$$\begin{aligned} \partial_{\hat{T}} A_1 = & -D_4 P^2 A_1 + P^2 \left( \frac{E_2 E_v}{3G} - F_2 P^2 \right) |A_1|^2 A_1 \\ & - \frac{5}{216} \frac{E_v^4}{G^3} |A_1|^4 A_1, \end{aligned} \quad (8)$$

where the coefficients

$$D = D_v + \eta^4 D_4, \quad E = E_v + \eta^2 E_2, \quad F = F_v + \eta^2 F_2 \quad (9)$$

have been expanded around the tricritical point

$$D_v = -GP^2, \quad E_v^2 = 6GF_v P^2. \quad (10)$$

Thus, the instability, which is signified by a sign change of the diffusion coefficient, need not always induce a phase slip, as it usually would in the Eckhaus instability. Instead, if  $\mathcal{D}(q)$  is negative in only a (small) region around a minimum, i.e. if  $F \equiv \frac{1}{2} \partial_q^2 \mathcal{D}(q)$  is sufficiently positive, the bifurcation becomes supercritical and the domain structures, which correspond to an oscillatory mode of the ‘particle in the potential’, are stable. In the subcritical case the domain structures persist up to the saddle-node given by

$$D_4 = \frac{6GP^4}{5E_v^4} (E_v E_2 - 3F_2 GP^2)^2. \quad (11)$$

To make contact with experiments [26], we model the diffusion coefficient  $\mathcal{D}(q)$  in the vicinity of a minimum in  $q$ ,

$$\begin{aligned} \mathcal{D}(R, q) = & \mathcal{D}(R_m, q_m) + \partial_R \mathcal{D} \cdot (R - R_m) \\ & + \frac{1}{2} \partial_q^2 \mathcal{D} \cdot (q - q_m)^2. \end{aligned} \quad (12)$$

At a Rayleigh number  $R$ , the parameters  $D, E$  and  $F$ , which are calculated by expanding  $\mathcal{D}(q, R)$  around the periodic solution at wave number  $q_0$ , are then given by

$$\begin{aligned} D = & \partial_R \mathcal{D} \cdot (R - R_m) + \frac{1}{2} \partial_q^2 \mathcal{D} \cdot (q_0 - q_m)^2, \\ E = & \partial_q^2 \mathcal{D} \cdot (q_0 - q_m), \quad F = \partial_q^2 \mathcal{D}. \end{aligned} \quad (13)$$

Here we have chosen  $R_m$  such that  $\mathcal{D}(q_m, R_m) = 0$ . A typical phase diagram for such a case is sketched in fig.3a. The thin line denotes the onset of the instability, whereas the thick lines give the locus of the saddle nodes. When raising  $R$  the instability first appears at  $q_m$  and is supercritical. Just before the transition the phase diffusion coefficient is still positive but it is very small over some range of wave numbers, thus irregularities in the structure are expected to decay very slowly. For larger  $R$  and consequently away from the minimum the bifurcation becomes subcritical. The width  $\delta q = 2P \sqrt{6G/\partial_q^2 \mathcal{D}}$  of the supercritical regime depends on the length  $L \equiv 2\pi/P$  of the system and vanishes as  $L \rightarrow \infty$ . In the subcritical regime, there exist two different domain structures in the region between the Eckhaus instability and the saddle-node line, one of which is unstable. This is related to the result of Brand and Deissler who find two different solutions of this type numerically [20].

In convection experiments in a very narrow channel Hegseth *et al.* have found stable domain structures with different wave numbers [26]. Brand and Deissler [16] suggested that they are related to the solutions discussed above, a position that is supported by the present results. When raising the Rayleigh number Hegseth *et al.* find a transition to domains, which can be supercritical or subcritical, depending on the average wave number  $q_m$ . Their results are shown in fig.3b for comparison with the predictions by the phase equation. This figure plots the maximum and minimum wave numbers of the pattern as the Rayleigh number is increased for two patterns which differ in their initial, homogeneous wave numbers. If the initial wave number is close to  $q_m$  there is a smooth (supercritical) transition to a domain structure as indicated by the circles. On the other hand, if the initial wave number is far from  $q_m$ , the periodic pattern persists to much higher values of the Rayleigh number and then jumps to the domain structure. The data for this case is shown by the squares and is indicative of a subcritical bifurcation.

Near  $q_m$  and  $R_m$ , our analysis suggests that phase diffusion should become very slow. This agrees with the experimental finding that the domain structures do not relax to a periodic pattern within the observational time scale when  $R$  is decreased just below  $R_m$  [26,30]. From the above discussion the diffusion coefficient  $\mathcal{D}(q)$  is expected to have a bimodal shape in  $q$  and a minimum at  $(R_m, q_m)$ , and to go through zero linearly in  $R$  there. This could be tested experimentally with methods similar to those used by Wu and Andereck in Taylor vortex flow [5].

Within the framework of the phase equation the interaction between domain walls is purely attractive [31]. Therefore, in regimes in which the phase equation applies domain walls annihilate each other as long as this is com-

patible with phase conservation. Thus, if the boundary conditions enforce phase conservation, the system will eventually reach a state with only a single domain-wall pair. If the boundary conditions do not conserve phase, e.g. in the presence of subcritical ramping in the control parameter  $R$  [33,8], domain structures exist only as transients [16,19]. In general, however, the interaction may also be repulsive, allowing domain-wall pairs to be stable without phase conservation. Such a situation can arise near threshold. It is examined in section IV using the Ginzburg-Landau equation which is introduced in the next section.

### III. DOMAIN STRUCTURES WITHIN A FOURTH-ORDER GINZBURG-LANDAU EQUATION

Close to threshold domain structures can arise if the basic state becomes unstable with respect to two patterns with different wave numbers, i.e. if the neutral curve for the appearance of a pattern has two minima. If the wave numbers are close to each other, such a system can be described by a single Ginzburg-Landau equation. It should be emphasized that in addition the minima must be due to the same mode. This is the case, for instance, in parametrically driven standing waves [17,27]. Such a Ginzburg-Landau equation is fourth-order in space, reflecting the two minima of the neutral curve,

$$\partial_{\tilde{T}} \tilde{A} = \tilde{D}_2 \partial_{\tilde{X}}^2 \tilde{A} + i \tilde{D}_3 \partial_{\tilde{X}}^3 \tilde{A} - \tilde{D}_4 \partial_{\tilde{X}}^4 \tilde{A} + \tilde{\Sigma} \tilde{A} - \tilde{\Gamma} |\tilde{A}|^2 \tilde{A}. \quad (14)$$

The convective amplitude  $\tilde{A}$  gives a typical quantity, e.g. the vertical velocity in convection, via

$$\tilde{v}_{\tilde{z}}(\tilde{x}, \tilde{z}, \tilde{t}) = \delta e^{i\tilde{q}_c \tilde{x}} \tilde{A}(\tilde{X}, \tilde{T}) f(\tilde{z}) + h.o.t. + c.c. \quad (15)$$

where  $\tilde{X} = \delta \tilde{x}$  and  $\tilde{T} = \delta^4 \tilde{t}$  are slow variables,  $\delta \ll 1$ , and  $f(\tilde{z})$  is the appropriate vertical eigenfunction. In order for (14) to be asymptotically valid  $\tilde{D}_2 \partial_{\tilde{X}}^2 \tilde{A}$  and  $i \tilde{D}_3 \partial_{\tilde{X}}^3 \tilde{A}$  have to be of the same order as  $\tilde{D}_4 \partial_{\tilde{X}}^4 \tilde{A}$ . Periodic solutions of this Ginzburg-Landau equation and their stability have been studied by Proctor [34].

In the following we solve (14) numerically for a finite system of length  $\tilde{L}$  with periodic boundary conditions. We are interested in particular in the behavior of the domains when the wave-number gradients become steep. To achieve this we scan across the full instability regime of the *periodic* pattern by changing the average wave number of the domain structure. To this end we investigate the dependence of the system on its length  $\tilde{L}$ . To keep  $L$ , the nondimensionalized system length, as a parameter we scale lengths using the critical wave number  $\tilde{q}_c$  rather than  $\tilde{L}$ ,

$$\tilde{X} = X/\tilde{q}_c, \quad \tilde{q} = \tilde{q}_c(1 + \delta Q), \quad \tilde{L} = L/\tilde{q}_c,$$

$$\begin{aligned} \tilde{A} &= A \tilde{q}_c^2 \sqrt{\tilde{D}_4/\tilde{\Gamma}}, \quad \tilde{T} = T/(\tilde{D}_4 \tilde{q}_c^4), \\ \tilde{D}_2 &= D_2 \tilde{D}_4 \tilde{q}_c^2, \quad \tilde{D}_3 = D_3 \tilde{D}_4 \tilde{q}_c, \quad \tilde{\Sigma} = \Sigma \tilde{D}_4 \tilde{q}_c^4. \end{aligned} \quad (16)$$

With this scaling the Ginzburg-Landau equation becomes

$$\partial_T A = D_2 \partial_X^2 A + i D_3 \partial_X^3 A - \partial_X^4 A + \Sigma A - |A|^2 A. \quad (17)$$

Either  $D_2$  or  $\Sigma$  could still be scaled away, leaving the quantity  $D_2^2/\Sigma$  as the primary control parameter. We have chosen to retain both parameters to simplify scanning each of them across zero. As pointed out by Tuckermann and Barkley, periodic boundary conditions for the physical quantities like  $\tilde{v}_{\tilde{z}}$  imply non-periodic boundary conditions for the amplitude  $A$  [35],

$$A(X+L)e^{iL/\delta} = A(X). \quad (18)$$

Thus the conserved slow phase is the total slow phase  $\Delta\Phi$  of the pattern, not only that of the slowly varying amplitude and is given by

$$\Delta\Phi = L + \delta \int_0^L Q dx. \quad (19)$$

For small  $\delta$ , changing the length has a very strong effect on the amplitude  $A$ , since small changes in the physical wave number  $\tilde{q}$  imply large changes in the reduced wave number  $Q$ . In particular, with these boundary conditions the reduced wave number can be scanned across 0 by changing the length of the system. With periodic boundary conditions on  $A$ , for which  $Q = \frac{2\pi}{L} \cdot n$ , this would not be possible.

The neutral stability curve and Eckhaus boundary for (17) are shown in fig.4 for  $D_3 = 0$  in the limit of infinite system length. The Eckhaus boundary is obtained by a linear stability analysis of the periodic solution  $A = A_1 e^{iQX}$  that yields the growth rate  $\sigma$  of sideband disturbances with wavenumber  $Q \pm P$ ,

$$\sigma = -P^4 - (D_2 + 6Q^2)P^2 - \Sigma + Q^2 D_2 + Q^4 \pm \sqrt{(\Sigma - Q^2 D_2 - Q^4)^2 + 4P^2 Q^2 (D_2 + 2(P^2 + Q^2)^2)}. \quad (20)$$

The Eckhaus curve is obtained from this in the limit  $P \rightarrow 0$ . In each of the two minima of the neutral curve the stability of the periodic pattern is governed by the usual Eckhaus criterion. Note that for  $Q = 0$ , i.e. at the local maximum of the neutral curve, the periodic pattern is unstable for *all*  $\Sigma$ . The width of this unstable region is  $\Delta Q = \sqrt{-D_2}/6$ . The term ‘‘inner Eckhaus boundary’’ used below will refer to those parts of each Eckhaus boundary for which  $|Q| < |Q_{min}|$ , while ‘‘outer Eckhaus boundary’’ will refer to those parts for which  $|Q| > |Q_{min}|$ , where  $Q_{min} = \pm \sqrt{-D_2/2D_4}$  are the minima of the neutral-stability and Eckhaus curves.

In a finite system there is no longer a continuum of allowed wave numbers, instead there is a discrete spectrum  $\{Q_n\}$  of them. This also implies that  $P$  is quantized in a

similar manner. Using the chosen scaling (16),  $P$  is constrained to integer multiples of  $\frac{2\pi}{L}$ . In this case all allowed periodic solutions can be stable. Eq.(20) shows that for this to occur it is necessary that the wave numbers are spaced widely enough to straddle the unstable region in the center, i.e.  $D_2/P^2 > -5/2$ , and sufficient that  $Q = 0$  itself is stable, which happens for  $D_2/P^2 > -1$ . The latter is the case if the adjacent allowed wave numbers  $Q = \pm 2\pi/L$  lie outside the neutral curve. Again, a periodic solution that is unstable at onset retains its instability for all values of  $\Sigma$ .

Keeping  $D_2$  fixed, we have as control parameters the total slow phase of the system  $\Delta\Phi$ , the system length  $L$ , and  $\Sigma$ , which can be considered a reduced Rayleigh number. The domains are characterized by the difference  $\Delta Q$  between the largest and the smallest wave number in the solution which thus serves as an order parameter (cf. fig.1).

The previous work done on the phase equation (cf. sec.II) gives some indication of what to expect in these simulations. For large  $\Sigma$  and small  $D_2$  the phase equation (3), and therefore its amplitude equation (8), is valid. In that region of parameter space it is expected that a branch of unstable domain structures bifurcates from the inner Eckhaus boundary and undergoes a saddle-node bifurcation to a branch of stable domain structures (cf. fig.3). On the other hand, for values of the parameters near the minimum of the neutral-stability curve, the solutions can be described using the phase equation appropriate to the typical Eckhaus case. Thus it is expected that there is an unstable branch that bifurcates subcritically from the inner Eckhaus boundary and combines with an unstable branch bifurcating subcritically from the outer Eckhaus boundary. In the following we concentrate on the transition region between these two types of behavior.

To calculate domain structures and examine their stability we solve the Ginzburg-Landau equation (17) with boundary conditions (18) numerically. The solutions are found using Newton's method and their stability is determined using inverse iteration. The average reduced wave number  $\bar{Q} = \int_0^L Q dx/L$  is used as a control parameter. To change this it is most straightforward to alter  $L$  by changing the grid spacing  $dx$  ( $\approx 0.25$  in this section). The additional parameters are given by  $\Delta\Phi \approx 113.7$ ,  $\delta = 0.1$ ,  $D_2 = -1.0$  and  $\Sigma$  chosen as indicated. We concentrate on the symmetric case  $D_3 = 0$ .

A set of four solutions at representative values of the two control parameters are shown in fig.5. The average reduced wave number  $\bar{Q}$  remains constant in the columns while  $\Sigma$  remains constant in each row. The local wave number is marked by the heavy solid line, whereas  $Re(e^{iq_c x} A)$  with  $q_c = 1$  is denoted by the thin line. As is apparent in fig.5a,c the dominant effect of increasing the average wave number  $\bar{Q}$  is a decrease in the length of the low-wave number region in the center. A striking feature, which is particularly important in the next section is demonstrated in fig.5a,b; the local wave number is non-

monotonic and exhibits spatial oscillations. These oscillations become increasingly pronounced with decreasing  $\Sigma$ . We will comment on the relevance of this below.

A sequence of bifurcation diagrams displaying the transition from the large- $\Sigma$  to the small- $\Sigma$  behavior is given in fig.6. In fig.6a  $\Sigma = 1.2$ . The branch of the stable domain structure is indicated by the bold line terminating in the saddle-node bifurcation  $A$  at  $\bar{Q} \approx 0.68$ . There it collides with an unstable branch of solutions that bifurcates off the periodic solution ( $\Delta Q = 0$ ) at the inner Eckhaus boundary (cf. fig.4 at  $\bar{Q} \approx 0.43$ ). The dotted line represents another branch of unstable solutions that arises from the outer Eckhaus boundary ( $\bar{Q} \approx 1.12$ ) and undergoes a phase slip as  $\bar{Q} \rightarrow 0$  which changes  $\Delta\Phi$  by  $2\pi \cdot \delta$ .

Lowering the control parameter  $\Sigma$  to 1.0, introduces new features (fig.6b). The original saddle-node bifurcation  $A$  remains, but two new saddle-node bifurcations,  $B$  and  $C$ , have appeared in the stable branch. These new saddle nodes mark the ends of a loop that grows as  $\Sigma$  is reduced. In going through the loop, the wave number changes from having a local maximum and two local minima in the low-wave-number domain (as in fig.5b) to having only a single minimum in that domain. Additionally, the branch from the outer Eckhaus boundary moves closer to the stable solution branch.

Reducing the parameter to  $\Sigma = 0.9$  (fig.6c) produces significant changes in the bifurcation diagram. The outer Eckhaus branch merges with the branch of stable domain solutions to produce two new saddle nodes,  $D$  and  $E$ . As  $\Sigma$  is lowered further, the saddle-node pairs  $C$  and  $D$  as well as  $A$  and  $E$  move together (fig.6d) and annihilate leaving only one surviving saddle node,  $B$ .

Lowering  $\Sigma$  to 0.3 produces no qualitative change in the behavior of the system. There continues to be only a single saddle node, at the tip of the loop (fig.6e). An additional (dashed) line is indicated in this figure. It represents another solution branch that undergoes a phase slip of  $4\pi \cdot \delta$  as  $\bar{Q} \rightarrow 0$ . Comparing this analysis with that of the phase equation (3) it is tempting to associate this branch with a phase perturbation  $\phi$  of wave number  $P = \frac{2\pi}{L} \cdot 2$  (cf. (7)). It is therefore expected to merge with the periodic solution for large  $\bar{Q}$ . We were, however, unable to continue it that far, since additional saddle-node bifurcations arise. In the wave-number region of interest, it merges with the branch of stable domain structures between  $\Sigma = 0.3$  and  $\Sigma = 0.25$  producing two new saddle-node bifurcations,  $F$  and  $G$ , shown in fig.6f. The latter annihilates with saddle node  $B$  around  $\Sigma = 0.2$ . Upon lowering  $\Sigma$  further, additional saddle nodes form and annihilate pairwise. This is presumably due to the interaction with additional branches corresponding to phase slips  $2\pi \cdot \delta \cdot n$ ,  $n > 2$ .

The above numerical results yield the phase diagram shown in fig.7. This picture shows one half of the parameter space and is symmetrically continued for  $Q < 0$ . Stable domain structures exist in the region above and

to the left of the line formed by the solid circles. Each of them indicates a saddle-node bifurcation of the stable branch. Above  $\Sigma \approx 1.2$  there exists only a single line of saddle-node bifurcations ( $A$ ). The first line of new dots ( $B$  and  $C$ ), to the left of line  $A$  denotes the loop first shown in fig.6b. The two saddle nodes in the loop are so close together that they cannot be resolved in this figure. For smaller  $\Sigma$  ( $\approx 1.0$ ), a hump arises from the creation of saddle nodes  $D$  and  $E$ , at the merging of the stable branch with the  $2\pi$ -phase-slip branch. These saddle nodes annihilate pairwise, leaving only one ( $B$ ). At  $\Sigma \approx 0.3$  another hump appears, caused by the merging of the  $4\pi$ -phase-slip branch and the branch of stable domain structures, creating saddle nodes  $F$  and  $G$ . Again, two of the saddle nodes merge and annihilate leaving only one. Similar humps that appear in the saddle-node line suggest that this process continues as  $\Sigma$  is reduced and  $\bar{Q}$  approaches zero.

The phase equation breaks down when the local wave number approaches the neutral curve. As fig.7 shows we have been able to find stable domain structures for values of  $\Sigma > -0.177$ . In this regime, the wave number is locally below the neutral curve. Thus the domain structures exist and are stable well beyond the validity of the phase equation. Strikingly, this leaves no trace in the stability properties of the domain structure. It is, however, responsible for the oscillatory behavior of the wave number (cf. fig.5). It is not clear whether or not the domain structures exist all the way to the minimum of the neutral curve, occurring at  $\Sigma = -0.25$ .

For simplicity we have concentrated on the special case  $D_3 = 0$  [36]. If  $D_3 \neq 0$  then one of the two minima in the neutral curve is lower than the other. Thus, if the control parameter is raised adiabatically, domain structures will not arise spontaneously from the basic state as the critical parameter value is crossed. Instead a periodic pattern with a wave number corresponding to the lower minimum will arise. If, however, the control parameter is quenched into the region in which there are two separate stable regions, then domain structures are expected to form. As shown by Proctor [34], the region of stable wave numbers that arises at the higher value of the control parameter is closed at the top rather than open as is the case here. We do not expect this to have a strong effect, however, in the regions of parameter space under investigation here.

#### IV. DOMAIN STRUCTURES WITHOUT PHASE CONSERVATION

Within the phase equation the dynamics of domain structures depends sensitively on the boundary conditions. In particular, the stability of a domain structure consisting of a single domain-wall pair requires the boundary conditions to conserve the phase. It is therefore of interest to study which properties of such a domain structure are independent of the boundary conditions

within the Ginzburg-Landau equation. This information will also give insight into the properties of domain structures consisting of many domain walls. In such structures adjacent domain-wall pairs can annihilate even if the total phase is conserved since nearby domains can grow or shrink to compensate for the loss of phase.

To investigate the behavior of domains in such a situation we use the fourth-order Ginzburg-Landau equation introduced in the previous section. Boundary conditions which do not conserve the phase can be obtained by introducing a smooth subcritical ramp in the control parameter  $\Sigma$  at each end of the system [33,8]. Since the amplitude at each end of the system goes then to zero, phase can be added or removed through the boundaries. Effectively, a ramp poses boundary conditions on the wave number [33,8]. In this system it selects either of the two minima of the neutral curve  $\pm Q_{min}$ . Since these wave numbers are consistent with the wave numbers found inside each domain, the ramps mimic the effect of distant domain structures.

To simulate the time evolution numerically we use a Crank-Nicholson scheme with  $dx \approx 0.034$  and  $nx = 3200$ . The weakness of the attraction between domain walls suggested such a small grid spacing to eliminate pinning by the lattice points. The initial conditions for all of the simulations performed in this section consist of a step function with three domains, two of high wave number surrounding one of low wave number. The initial conditions are varied by changing the width of the central (low wave number) domain.

In order to confirm that this ramping is sufficient to eliminate phase conservation, we start by investigating large values of the control parameter,  $\Sigma = 100$  (with  $D_2 = -1.0$ ). In this region of parameter space, the phase equation governs the dynamics of the pattern and the domain walls will have purely attractive interaction. As expected, all of the different initial conditions tested converged to a periodic pattern with wave number  $Q_{min}$ . This shows in addition that the numerical parameters selected are sufficient to eliminate pinning on the grid in this regime.

We next consider the behavior of domains for lower values of the control parameter  $\Sigma$ . These simulations were performed for  $\Sigma = 1.0$  and  $D_2 = -1.0$ . For these values of the control parameter, close to the neutral-stability curve, the dynamics is no longer expected to be governed by the phase equation. The behavior is indeed quite different from that observed for high  $\Sigma$ . Here the system evolves to a discrete number of different states, as shown in fig.8, where the total phase in the system (between the ramps) is plotted versus time. As the initial width of the central (low wave number) domain is increased, the total phase of the initial condition is decreased, leading to the different lines shown in this plot. The upper lines are those with only an initially narrow region of low wave numbers. They converge to a final state with a single minimum in wave number. The next set of lines have a slightly wider region of low wave number and converge

to a final state with two minima in the wave number. Likewise the lowest set of lines converge to a state with three minima in the wave number. The corresponding final states are shown in fig.9. These results show that the width of the domain structures is quantized and the final states can be characterized by the number of minima in the wave number.

We now turn to the transition region between the low- $\Sigma$  regime, where domain structures exist, and the large- $\Sigma$  regime, where they do not. In the next section, we will relate the stability regime of domain structures to that of zig-zag patterns in two-dimensional systems. For that application it is more natural to change  $|D_2|$  than  $\Sigma$  since the former is directly related to the roll-spacing of an initial straight-roll pattern. These two control parameters are equivalent since (17) has only a single control parameter, the ratio  $D_2^2/\Sigma$ . We therefore study the dependence on  $D_2$  instead of on  $\Sigma$ .

In order to determine the value of the control parameter at which the various states disappear, we create initial conditions consisting of domain structures with different widths for  $D_2 = -1.0$  and  $\Sigma = 1.0$ . Then  $D_2$  is increased adiabatically and a new steady solution is determined using Newton's method. The values of  $D_2$  and the total phase  $\Delta\Phi$  are recorded for each step. Figure 10 summarizes these results, plotting  $\Delta\Phi$  against  $D_2$ . As  $D_2$  is increased, the total phase in each state decreases. This is mainly because, the wave number in each of the domains,  $Q_{min}$ , decreases in absolute value as  $|D_2|$  decreases while the length of the domains stays essentially fixed. Eventually, each domain structure vanishes through a saddle-node bifurcation. These bifurcations occur at different values of the control parameter for different size domains. The value of  $D_2$  at which the bifurcation occurs increases for the domains with one to four minima and then decreases again for the state with five minima. The investigation of larger domains was not feasible with our finite difference code.

In the region of parameter space where the domain structures are stable, the interaction between the domain walls must change sign as a function of their distance. In principle, at large distances this interaction can be described using perturbation methods on heteroclinic orbits [37,38] and in simpler systems it has been shown that a spatially oscillatory behavior of the domain wall can lead to a locking of adjacent walls [37]. The asymptotic behavior of the solution far away from the domain wall can be determined through a linearization around the corresponding periodic solution of (17). For the periodic solution with wave number  $Q_{min}$  such an analysis reveals spatially oscillatory eigenmodes, but also modes that decay monotonically in space [32]. Correspondingly, in the numerical simulations the wave number is clearly a combination of oscillatory and monotonic decaying functions for small  $|D_2|$ . Thus, for adjacent domain walls to lock into each other the existence of an oscillatory mode is not sufficient; it has to dominate the monotonic mode.

At  $D_2 \approx -0.35$  the spatial decay rates of the two

modes are the same (for  $\Sigma = 1.0$ ). For larger  $D_2$ , the decay rate of the monotonic eigenmode is lower and it will dominate the oscillatory mode so the dynamics will be that predicted by the phase equation. For  $D_2 < -0.35$  the oscillatory mode has a smaller decay rate than the monotonic mode so repulsive as well as attractive interaction is possible. The oscillations are clearly illustrated in fig.5a,c where it is apparent that raising  $\Sigma$  (lowering  $D_2$ ) makes the oscillations near the domain wall much stronger. This argument suggests that domain structures could exist up to  $D_2 \approx -0.35$  and that wide ones persist to smaller values of  $|D_2|$  than narrow ones. This would be in agreement with the results for the states with one to four minima, but it does not explain the behavior of the five-minima state. Thus, a complete understanding of the numerical result seems to require a detailed calculation of the interaction.

The locking described in this section does not occur within the fourth-order phase equation (3) despite the presence of the fourth derivative. As eq.(5) shows the phase equation is effectively only second order when considering steady solutions. If a sixth-order term  $H\partial_X^6 Q$  were kept in the phase equation, oscillatory behavior of the wave number could be described by the phase equation for sufficiently large  $H$ . For this situation to be asymptotically valid both  $D$  and  $G$  have to be vanishingly small at the same time, which is, however, not to be expected in a typical physical system.

## V. DOMAIN STRUCTURES IN TWO-DIMENSIONAL SYSTEMS: ZIG-ZAGS

The results discussed in this paper can be extended to describe certain aspects of two-dimensional patterns. A common instability of two-dimensional roll patterns is the zig-zag instability. It leads to an undulatory deformation of the pattern along the rolls. During the nonlinear evolution the undulations become steeper and domains of parallel rolls arise. They are separated by domain walls within which the orientation of the rolls changes rapidly. Thus, they can be characterized by a wave vector  $(q_x, q_y)$  with  $q_y$  positive and relatively constant in a 'zig'-region and negative in a 'zag'-region. The behavior of  $q_y$  is therefore very similar to that of  $Q$  in the domain structures. Single domain walls between zigs and zags have been studied previously [47]. Here we concentrate on *pairs* of domain walls, which form a domain structure, and the interaction between them.

In isotropic systems, such as Rayleigh-Bénard convection, the zig-zag instability arises generically when the wave number becomes too small, since the zig-zag pattern leads to an increase in the local wave number. While these patterns have not been observed to saturate in Rayleigh-Bénard convection [48], numerical simulations [28] suggest that they can be stable in chemical systems [39,40].

Zig-zag patterns are also of great importance in anisotropic systems such as electro-hydrodynamic convection in nematic liquid crystals. There the long molecules exhibit a preferred direction and thus define an axis of anisotropy of the fluid. In these systems there are two possible primary bifurcations to roll-like structures. The first is to a parallel-roll pattern, in which the rolls are oriented normal to the axis of anisotropy and have wave vector  $(q_x, 0)$ . Such a pattern is therefore commonly referred to as a “normal-roll” pattern. The second type of primary bifurcation is to rolls oriented at an angle to the director. Due to reflection symmetry, such rolls can be oriented in two directions with wave number  $(q_x, \pm q_y)$ . This allows the formation of zig-zag patterns [29].

In a simplifying approach, it is possible to describe zig-zag-patterns using the phase equation (5) with  $Q$  corresponding to  $q_y$  [41,42,43]. Thus, only variations in  $q_y$  are considered, while  $q_x$  is taken to be constant. As discussed above, such a description contains in general no stable zig-zag structures; instead there is a coarsening of the pattern until there are no domain walls left and the pattern consists of only one type of rotated rolls. Only if the boundary conditions enforce phase conservation, there will be a single domain wall left (a pair of domain walls for periodic boundary conditions) which corresponds to a ‘zig-zag’-structure (‘zig-zag-zig’-structure for periodic boundary conditions).

In two-dimensional experimental systems the total phase is usually not conserved. It is therefore again of interest to investigate the stability of zig-zags in the absence of phase conservation. Thus, we consider the appropriate Ginzburg-Landau equation. For isotropic systems (as in Rayleigh-Bénard convection) it is given by [44],

$$\partial_T A = -(i\partial_X + \partial_Y^2)^2 A + \lambda A - |A|^2 A, \quad (21)$$

while for anisotropic systems (as in convection in nematics) it reads [45],

$$\partial_T A = (\partial_X^2 - iZ\partial_X\partial_Y^2 + W\partial_Y^2 - \partial_Y^4)A + \lambda A - |A|^2 A. \quad (22)$$

In the anisotropic case, the Lifshitz point, at which the pattern at onset changes from normal to oblique rolls, is given by  $W = -ZQ_x$ .

Concentrating on solutions which are strictly periodic in  $X$ ,  $A = A_1(Y, T)e^{iQ_x X}$ , one obtains eq.(17) with

$$D_2 = 2Q_x, \quad \Sigma = \lambda - Q_x^2 \quad \text{for (21)} \quad (23)$$

$$D_2 = W + ZQ_x, \quad \Sigma = \lambda - Q_x^2 \quad \text{for (22)}. \quad (24)$$

Note that  $Y$  and  $Q_y$  in the two-dimensional systems correspond to  $X$  and  $Q$  in eq.(17) and that now periodic boundary conditions for the physical quantities imply periodic boundary conditions for  $A_1$ . Thus, the domain structures discussed in sec.III are indeed one-dimensional analogs of zig-zag patterns.

Zig-zag patterns have been studied in some detail for anisotropic systems [45,41,42,43]. These studies found that there is no continuous transition from normal rolls to zig-zags of small amplitude. For sufficiently large amplitude, however, stable zig-zags are found to exist in islands within parameter space. Within these islands, the zigs and zags always orient themselves in the direction of maximal growth rate. Presumably these islands are related to the discrete set of domains with different widths discussed above.

Our results suggest a mechanism to explain the existence of these islands of stability. As eqs.(21-24) show, these results apply to both the anisotropic and the isotropic case. The implications of the results shown in fig.10 are presented in figs.11a-c. There the loci of the saddle-node bifurcations of the different domain states are given in the  $\lambda - Q_x$ -plane (medium-weight lines). These are the lines with  $D_2^2/\Sigma = \text{constant}$ , where the appropriate constant for each domain structure is obtained from fig.10. In addition the Eckhaus curve and the onset of the zig-zag instability are pictured. The figures differ in the values of  $Z$  and  $W$ , with fig.11(b) corresponding to the isotropic case. In each figure, the behavior of the patterns is similar. Between the Eckhaus instability (thin dotted line) and the zig-zag instability (thin dashed line) straight-roll patterns are stable. As the zig-zag instability is crossed they become unstable to undulations. Close to the onset of the instability the coarsening dynamics predicted by the phase equation will be observed. This results in a pattern that will eventually consist of oblique rolls in only one direction. Their wave number will be close to that with maximal growth rate and they will be stable.

If, however, the pattern is quenched deeper into the zig-zag-unstable regime the resulting zig-zag pattern will be able to persist, as the oscillations in  $Q_x$  can lock into one another. The analysis of the spatial decay rates suggests that it is necessary to quench at least beyond the thickest solid line, which corresponds to  $D_2 < -0.35$ . The numerical results indicate one has to quench all the way beyond the medium-weight solid line, which corresponds to the four-minima state to find stable zig-zags. The different medium-weight lines denote the stability limits of ‘zig-zag-zig’ structures with different lengths of the ‘zag’-domain. Note that these lines merge with the line denoting the zig-zag-instability on the neutral curve (thin solid line). Except for  $W = 0$  the merging occurs therefore at wave numbers for which the straight rolls are unstable with respect to the Eckhaus instability. Consequently, for small  $\lambda$  stable, locked domain structures arise only at wave numbers  $Q_x$  for which the straight rolls are unstable. Although the Eckhaus-instability of straight rolls does not necessarily imply that of the zig-zag-structures, it points to the importance of instabilities which involve the  $X$ - as well as the  $Y$ -dependence and suggests that these may be of particular importance for small  $\lambda$ . In our analysis there is no allowance for such two-dimensional instabilities. For some of the domain

structures they have been investigated in the anisotropic case [45,41,42,43]. In these studies stable zig-zag structures have been found in certain parameter regimes.

A typical ‘zig-zag-zig’ solution is illustrated in fig.12a for  $D_2 = -1$  and  $\Sigma = 0$ . It takes the one-dimensional pattern  $A(X)$  shown in fig.12b and extends it into two dimensions by plotting  $Re(A(X)e^{iQ_y Y})$  with constant  $Q_y = 0.7$ . The lines represent the zeroes of the pattern, while the dark spots are maxima and minima. This pattern is stable. A signature of the oscillations in  $Q_x$  is the appearance of undulatory deformations in the zig-zag structure near the domain walls.

## VI. CONCLUSION

We have considered two approaches to investigating the existence and stability of domain structures in pattern-forming systems: a phase equation and a Ginzburg-Landau equation. Within the phase equation the structures typically arise through a subcritical bifurcation. This approach yields qualitative agreement with various experimental results in slot convection [26]. As a conclusive test we suggest a measurement of the wave-number dependence of the phase diffusion coefficient  $\mathcal{D}(q)$ , which is expected to have a bimodal shape. The phase-equation approach becomes invalid when the transition region between adjacent domains becomes too narrow, i.e. when the gradient in wave number becomes too steep. This is in particular the case near onset.

In the second approach we used a Ginzburg-Landau equation to describe the competition between patterns with different wave numbers close to onset. Such a competition naturally arises in a system with a double-welled neutral-stability curve, as is, for instance, possible in parametrically driven standing waves [17,18,27]. This approach allowed the investigation of domain structures and their stability even for large wave-number gradients. We found domain structures are stable over their entire region of existence. Strikingly this region is very intricate due to the interaction with unstable structures possibly arising from the outer Eckhaus boundary.

The domain structures exist well beyond the regime of validity of the phase equation. A characteristic feature of those which are not described by the phase equation is the oscillatory behavior of their wave number. This allows adjacent domain walls to lock into each other, forming domain structures which are stable even without phase conservation. We have numerically studied the dependence of their regime of stability as a function of the length of the domains.

Zig-zag patterns can be considered as two-dimensional analogs of domain structures. Therefore, in systems in which the phase is not conserved, they are not stable at onset of the zig-zag instability. Only further in the zig-zag-unstable regime can the locking prevent the pairwise annihilation of zigs and zags.

This work has been supported by grants from NSF/AFOSR (DMS-9020289, DMS-9304397) and DOE (DE-FG02-92ER14303). H.R. acknowledges interesting discussions with W. Pesch, L. Kramer, and E. Bodenschatz.

<sup>+</sup> present address: SCRI, Florida State University B-186, 400 Dirac Science Center Library, Tallahassee, FL 32306.

- 
- [1] P. Manneville, *Dissipative Structures and Weak Turbulence*, Academic Press, 1990.
  - [2] M.C. Cross and P.C. Hohenberg, *Rev. Mod. Phys.* 65 (1993) 851.
  - [3] V. Croquette and F. Schosseler, *J. Physique* 43 (1982) 1183.
  - [4] U. Gerdts, Ph.D. thesis, University of Kiel, 1985 (unpublished).
  - [5] M. Wu and C.D. Andereck, *Phys. Rev. A* 43 (1991) 2074.
  - [6] H. Riecke and H.-G. Paap, *Phys. Rev. Lett.* 59 (1987) 2570.
  - [7] M. Lücke and D. Roth, *Z. Phys. B* 78 (1990) 147.
  - [8] H.-G. Paap and H. Riecke, *Phys. Fluids A3* (1991) 1519.
  - [9] W. Eckhaus, *Studies in Nonlinear Stability Theory*, Springer, New York, 1965.
  - [10] L. Kramer and W. Zimmermann, *Physica* 16D (1985) 221.
  - [11] M. Lowe and J.P. Gollub, *Phys. Rev. Lett.* (1985) 2575.
  - [12] L. Kramer, H.R. Schober and W. Zimmermann, *Physica* 31D (1988) 212.
  - [13] E. Braun, S. Rasenat and V. Steinberg, *Phys. Rev. A* 43 (1991) 5728.
  - [14] M.A. Dominguez-Lerma, D.S. Cannell and G. Ahlers, *Phys. Rev. A* 34 (1986) 4956.
  - [15] H. Riecke and H.-G. Paap, *Phys. Rev. A* 33 (1986) 547.
  - [16] H.R. Brand and R.J. Deissler, *Phys. Rev. Lett.* 63 (1989) 508.
  - [17] H. Riecke, *Europhys. Lett.* 11 (1990) 213.
  - [18] H. Riecke, in *Nonlinear Evolution of Spatio-Temporal Structures in Dissipative Continuous Systems*, eds. F.H. Busse and L. Kramer, p.437, Plenum 1990.
  - [19] H.R. Brand and R.J. Deissler, *Phys. Rev. A* 41 (1990) 5478.
  - [20] R.J. Deissler, Y.C. Lee and H.R. Brand, *Phys. Rev. A* 42 (1990) 2101.
  - [21] C.D. Andereck, S.S. Liu and H.L. Swinney, *J. Fluid Mech.* 164 (1986) 155.
  - [22] I. Mutabazi, J.J. Hegseth, C.D. Andereck and J.E. Wesfreid, *Phys. Rev. Lett.* 64 (1990) 1729.
  - [23] B.W. Baxter and C.D. Andereck, *Phys. Rev. Lett.* 57 (1986) 3046.
  - [24] D. Bensimon, P. Kolodner and C.M. Surko, *J. Fluid Mech.* 217 (1990) 441; E. Moses, J. Fineberg and V. Steinberg, *Phys. Rev. A* 35, 2757 (1987); R. Heinrichs, G. Ahlers and D.S. Cannell, *Phys. Rev. A* 35, 2761 (1987).
  - [25] J.-J. Perraud, E. Dulos, P. De Kepper, A. De Wit, G. Dewel and P. Borckman, in *Spatio-Temporal Organization in Nonequilibrium Systems*, eds. S.C.Müller and T. Plesser, p.205, 1992.

- [26] J. Hegseth, J.M. Vince, M. Dubois and P. Bergé, *Europhys. Lett.* 17 (1992) 413.
- [27] H. Riecke, M. Silber and L. Kramer, *Phys. Rev. E* 49 (1994) 4100.
- [28] V. Dufiet and J. Boissonade, *J. Chem. Phys.* 96 (1992) 664.
- [29] R. Ribotta and A. Joets, *J. Physique* 47 (1986) 595.
- [30] M. Dubois, priv. comm.
- [31] K. Kawasaki and T. Ohta, *Physica* 116A (1982) 573.
- [32] D. Raitt, Ph.D. Thesis, Northwestern University, 1994 (unpublished).
- [33] L. Kramer, E. Ben-Jacob, H. Brand and M. Cross, *Phys. Rev. Lett.* 49 (1982) 1891.
- [34] M.R.E. Proctor, *Phys. Fluids A* 3 (1991) 299.
- [35] L. Tuckerman and D. Barkley, *Physica* 46D (1990) 57.
- [36] This is obtained in the one-dimensional description of two-dimensional systems, where the odd derivative vanishes due to reflection symmetry (see (21) and (22) below).
- [37] P. Coulet, C. Elphick and D. Repaux, *Phys. Rev. Lett.* 58 (1987) 5478.
- [38] C. Elphick, E. Meron and E.A. Spiegel, *SIAM J. Appl. Math.* 50 (1990) 490.
- [39] V. Castets, E. Dulos, J. Boissonade and P. DeKepper, *Phys. Rev. Lett.* 63 (1990) 2953.
- [40] Q. Ouyang and H.L. Swinney, *Nature* 352 (1991) 610; *Phys. Rev. Lett.* 64 (1990) 2953.
- [41] E. Bodenschatz, M. Kaiser, L. Kramer, W. Pesch, A. Weber, and W. Zimmermann, in *The Geometry of Non-Equilibrium* Eds. P. Coulet and P. Huerre, p.111, Plenum 1991.
- [42] L. Kramer, E. Bodenschatz, W. Pesch, and W. Zimmermann, in *The Physics of Structure Formation*, eds. W. Güttinger and G. Dangelmayr, Springer, Berlin, 1987.
- [43] E. Bodenschatz, Ph.D. Thesis, University of Bayreuth, 1989 (unpublished).
- [44] A.C. Newell and J.A. Whitehead, *J. Fluid Mech.* 38 (1969) 279; L.A. Segel, *J. Fluid Mech.* 38 (1969) 203.
- [45] W. Pesch and L. Kramer, *Z. Phys.* B63 (1986) 121.
- [46] D. Raitt and H. Riecke, in *Spatio-Temporal Patterns in Nonequilibrium Complex Systems*, eds. P.E. Cladis and P. Palfy-Muhoray, Addison-Wesley, (to appear).
- [47] B.A. Malomed, A.A. Nepomnyashchy and M.I. Tribelsky, *Phys. Rev. A* 42 (1990) 7244.
- [48] Recently, more complicated zig-zag patterns have been found to be stable in numerical computations of Rayleigh-Bénard convection: F.H. Busse and M. Auer, *Phys. Rev. Lett.* 72 (1994) 3178.

FIG. 1. Typical domain structure solution. The thick line gives the local wave number, while the thin line represents a typical physical quantity like the mid-plane temperature.

FIG. 2. Potentials  $U(q)$  for (a)  $F < 0$  ( $\mathcal{D}(q)$  concave down) (b)  $F > 0$  ( $\mathcal{D}(q)$  concave up).

FIG. 3. Comparison of (a) phase diagram obtained from the phase equation (8) with (b) experimental results obtained by Hegseth *et al* [26].

FIG. 4. Neutral stability and Eckhaus curves for  $D_2 = -1$  and  $D_4 = 1$ .

FIG. 5. Four solutions obtained at different values of the control parameters  $\bar{Q}$  and  $\Sigma$ . The local wave number is marked by the heavy solid line, whereas  $Re(e^{iq_c x} A)$  with  $q_c = 1$  is denoted by the thin line. The order parameter  $\Delta Q$  is also indicated.

FIG. 6. Bifurcation diagrams for various values of  $\Sigma$ : a)  $\Sigma = 1.2$ , b)  $\Sigma = 1.0$ , c)  $\Sigma = 0.9$ , d)  $\Sigma = 0.8$ , e)  $\Sigma = 0.3$ , f)  $\Sigma = 0.25$ . The branches of *stable* domain structures are denoted by thick lines. For details see text.

FIG. 7. Phase diagram: domain structures exist and are stable above and to the left of the saddle-node line denoted by solid circles. The letters denote the loci of the respective saddle-node bifurcations shown in fig.6. The dashed and thin lines give the neutral and the Eckhaus curves, respectively.

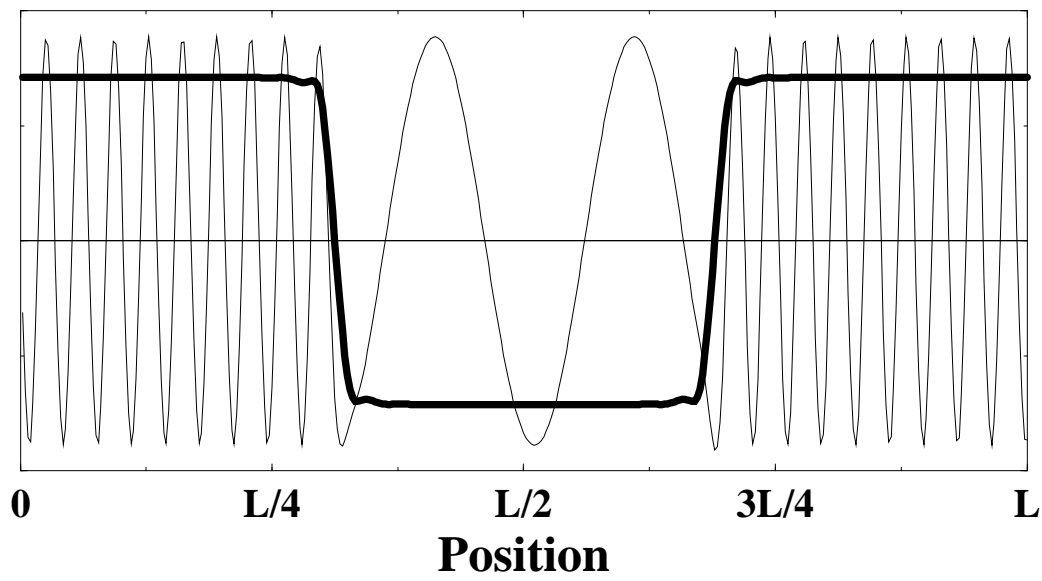
FIG. 8. Temporal evolution of the total phase for different initial conditions in the absence of phase conservation. The corresponding final states are shown in fig.9.

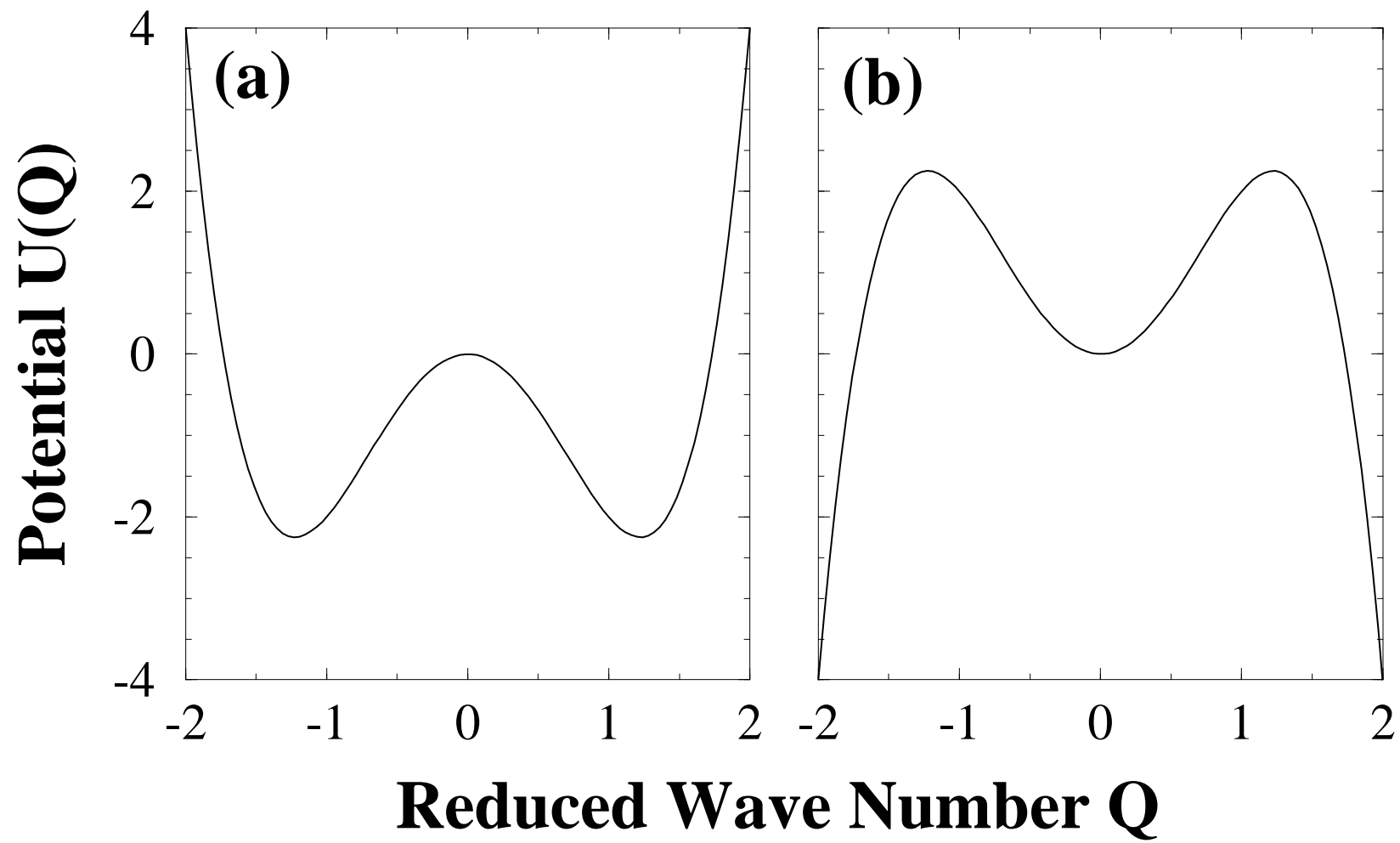
FIG. 9. Coexisting stable final states obtained from the time evolution shown in fig.8. The thick line gives the local wave number in the bulk. Note that the amplitude goes to zero toward the boundaries due to the subcritical ramping.

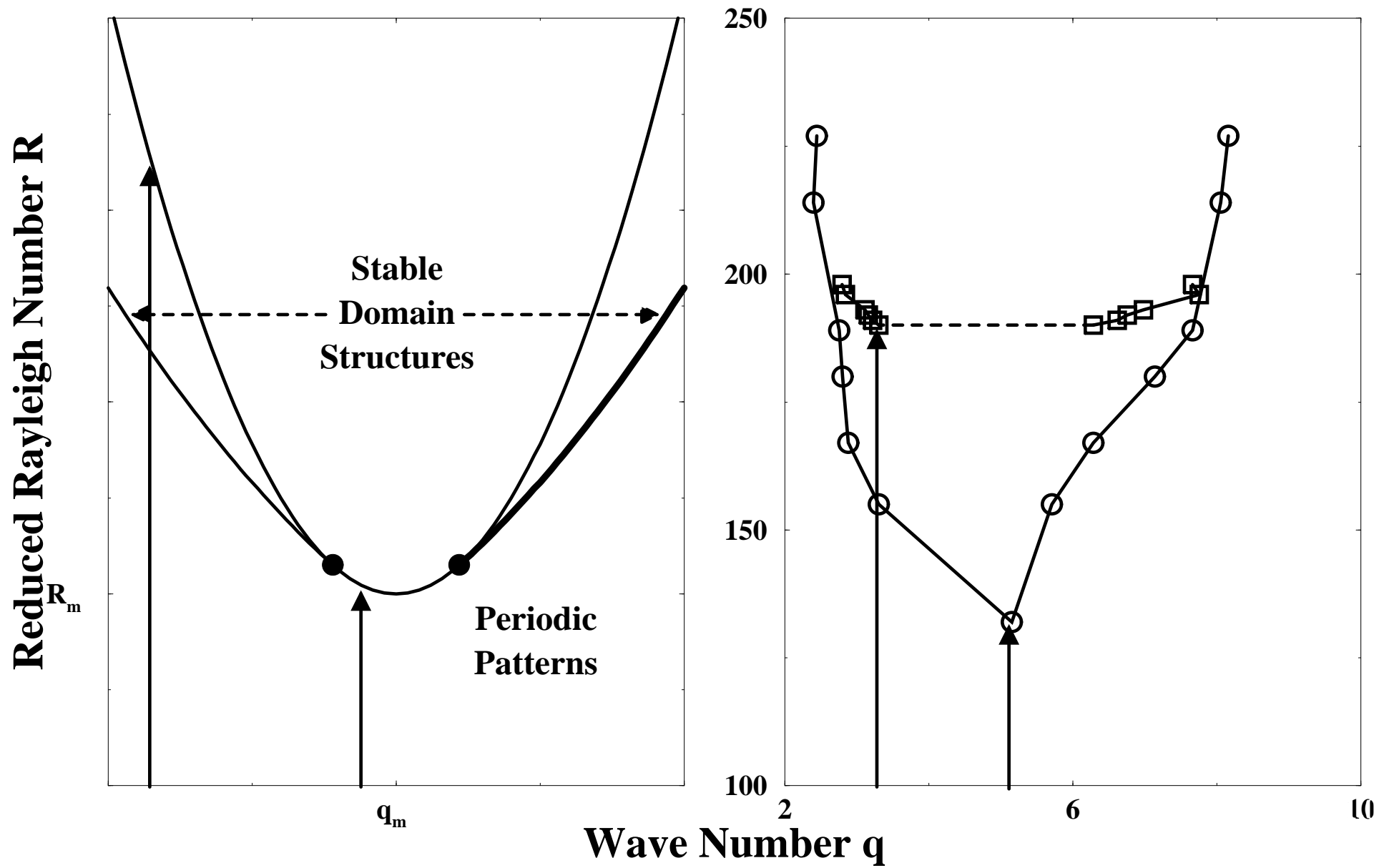
FIG. 10. Regime of existence of bound pairs of domain walls for  $\Sigma = 1$ . The calculation was performed with up to 25,600 points and an appropriate grid spacing down to  $dx \approx 0.016$ . The ramped part is up to 3,200 points wide on each side.

FIG. 11. Extension of one-dimensional results of fig.10 to zig-zag patterns for different values of  $W$  and  $Z$  in eq.(22), (a)  $W = -0.25$ ,  $Z = 1.5$ , (b)  $W = 0.0$ ,  $Z = 2.0$  (isotropic case), and (c)  $W = 0.25$ ,  $Z = 1.0$ . To the left of the medium-weight lines zig-zags of different widths are locked: four-minima state (solid), one-minimum state (dotted). At the thickest line the monotonic and the oscillatory mode have the same decay rate. Between it and the zig-zag instability (thin dashed line), there are no stable straight-roll or zig-zag solutions within this framework. Thin lines: neutral-stability curve (solid), Eckhaus instability (dotted). Between the zig-zag instability and the Eckhaus instability straight-roll patterns are stable.

FIG. 12. Two-dimensional analog of domain structure: zig-zag pattern (a) and the domain structure (b) from which it was generated. Both the wave number (thick line) and  $Re(Ae^{iq_c x})$  with  $q_c = 1$  (thin line) are shown in (b). The parameter values are  $\Sigma = 0$ ,  $D_2 = -1$ ,  $Q_y = 0.7$ .







# Reduced Rayleigh Number $\Sigma$

